A COMPUTER-CONTROLLED DIELECTRIC CONSTANT MEASUREMENT SYSTEM: THE MOVING VANE DIELECTOMETER

Q-4

Glen E. Everett
and
James W. Battles
Michelson Laboratory, Physics Division
Naval Weapons Center, China Lake, California 93555

ABSTRACT

A computer-controlled dielectric constant and data analysis system has been developed. Motion of a metallic vane in an inhomogeneously dielectric-filled rectangular wave guide system provides reflection coefficient versus effective sample length from which the dielectric constant is determined.

Introduction

The determination of complex dielectric constants, $\varepsilon = \varepsilon'(1 - j \tan \delta)$, at microwave and millimeter wavelength is based on measurement of the magnitude and phase of either a transmission or reflection coefficient of a sample in either a free space or "guided" wave configuration [1]. Reference 1 summarizes 30 methods which can be employed and discusses the conditions required for precision measurements. The short circuited line method, suitable for use with small samples and measurements versus temperature, is shown in Fig. 1a. The complex reflection coefficient, $\Gamma(\ell)$, is given by

$$\Gamma(\ell) = \frac{\Gamma(\infty) - e^{-2\gamma\ell}}{1 - \Gamma(\infty)e^{-2\gamma\ell}} \qquad (1)$$

where ℓ and γ are the sample length and complex propagation constant, respectively. The surface reflection coefficient,

$$\Gamma(\infty) = \frac{Z_d - Z_o}{Z_d + Z_o}, \qquad (2)$$

represents the limiting condition, $\gamma\ell >> 1$. The parameters $\Gamma(\infty)$ and γ are determined by ε' and tan δ as well as frequency and waveguide dimensions.

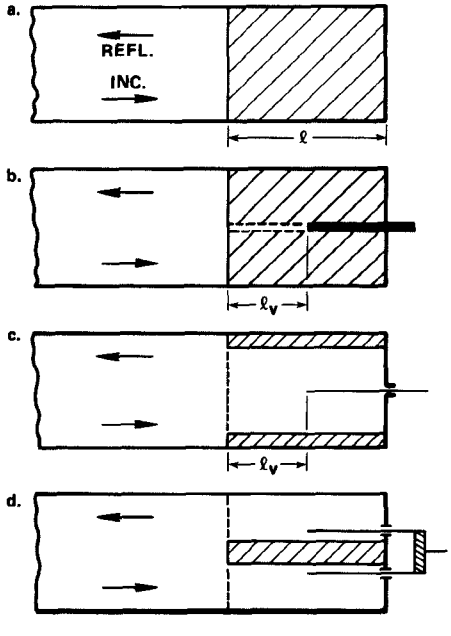

Fig. 1.

The reflection coefficient, $\Gamma(\ell)$, can be measured with a slotted line. The magnitude is determined from the VSWR and the phase from the position change of the standing wave minimum with respect to the empty waveguide. Accurate values of either ε' or tan δ can be determined, in principle, through the proper choice of sample length. In practice, the determination of ε' and tan δ is restricted to a limited range for these parameters. Experimental factors limiting accuracy are the finite size and reflection from the slotted line probe and detector deviations from a square law dependence. The latter is particularly important for the large VSWRs occuring with low loss (tan $\delta << 1$) materials. Additional uncertainties arrise from a gap between the sample and terminating short.

Moving Vane Dielectometer

The "Moving Vane Dielectometer" is shown conceptually in Fig. 1b. The conducting movable vane, surfaces parallel to the waveguide narrow walls, produces two waveguide sections behind the vane edge which are beyond cutoff for ε' not too large (this condition can be satisfied by decreasing the effective sample thickness as shown if Figs. 1c and 1d). The effective attenuation coefficient, α_c, in the cutoff region behind the vane approaches $\alpha_c \approx 54.6$ dB/unit length in the limiting case $(\lambda/\lambda_c) >> 1$ [2]. When the vane is long compared to the attenuation length, its impedance and reflection coefficient are independent of the cutoff region's termination characteristics. Neglecting dielectric losses at the vane interface, they can be represented by

$$Z_v = jZ_d \tan(\Phi_v/2)$$

$$\Gamma_v = e^{j\Phi_v}$$

The reflection coefficient as a function of effective sample length, ℓ_v (the region in front of the vane, Fig. 1b) becomes

$$\Gamma(\ell_v) = \frac{\Gamma(\infty) - e^{-(2\gamma\ell_v - j\Phi_v)}}{1 - \Gamma(\infty)e^{-(2\gamma\ell_v - j\Phi_v)}} \qquad (3)$$

Using either the split or centered geometry shown in Figs. 1c and 1d respectively, $\Gamma(\ell_v)$ can be measured as a continuous function of sample length, from which the complex dielectric constant can be determined using standard curve fitting procedures.

A block diagram of the measurement system for one of two identical channels is shown in Fig. 2. The vane for each channel is driven by a common stepper motor-lead screw assembly (not shown). Vane position is determined using a differential shaft angle encoder coupled to the lead screw. The encoder provides one count per motor step, i.e., 180 counts/rev. The balanced mixer output is proportional to

$$e_s(\ell,\Phi) = 4\,[\Gamma_r(\ell)\cos\Phi + \Gamma_i(\ell)\sin\Phi] \qquad (4)$$

where

$$\Gamma(\ell) = \Gamma_r(\ell) + j\,\Gamma_i(\ell)$$

and Φ is the phase difference between the reference and signal (empty) arms. A phase shifter in the reference arm (not shown) is set to 0° and $e_s(\ell,\Phi)$ is measured. A second measurement with the phase shifter at 90° gives $e_s(\ell,\Phi+\pi/2)$. The two measurements at each value of ℓ are combined to give the magnitude and phase of $\Gamma(\ell)$ as a function of ℓ.

The measurement system is interfaced to and controlled by a Hewlett-Packard Model 1000 F-Series computer. A special purpose interface providing stepper motor speed and direction control was developed for the system. It provides linear motor acceleration from 1 step/sec to 1000 steps/sec in one second following either a motor start or direction change signal. The balanced mixer outputs are connected to a multichannel 12-bit ADC which can provide up to 2×10^4 measurements/sec. In response to each stepper motor rotation pulse, each mixer channel is sampled and the results stored in the computer's main memory. The very small vane displacement increment and memory addressing restrictions require that data be taken in blocks. A start command from the computer initiates the stepper motor controller causing 8192 measurement steps. At the end of each data block, results are transferred to a magnetic disk file and the next measurement block initiated. The number of measurement blocks used is selected to provide a complete vane motion cycle, i.e., Min-Max-Min vane insertion positions.

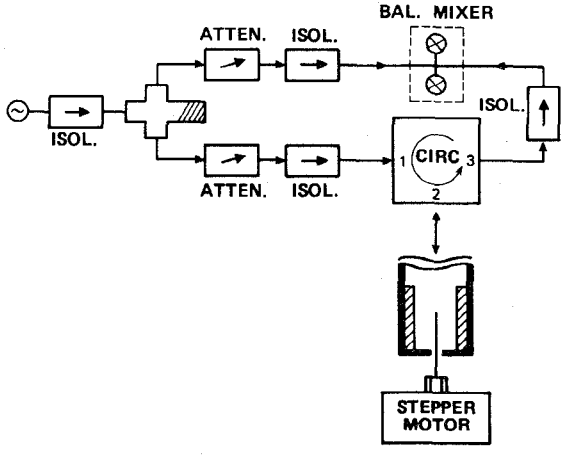

Fig. 2. System block diagram of one measurement channel. A phase shifter in the balanced mixer reference is not shown. In the actual system vane travel is from a lead screw driven by the stepper motor. The lead screw and differential shaft angle encoder are omitted for clarity.

The lead screw-stepper motor assembly (4,000 steps/in) at 1 kHz gives vane travel of 4 sec/in. The 6-inch Min-Max displacement corresponds to an ideal full cycle measurement time of 48 sec. At X-band the vane position change per step, $(\Delta\ell/\lambda_g) \simeq 0.4 \times 10^{-3}$, is smaller than justified by a 12-bit ADC. Data compression is effected by summing 16 contiguous measurements and storing the result as a single 16-bit word. Motor acceleration at a direction reversal or start of new block together with data compression and transfers to disk storage give actual measurement times of $\sim$ 60 sec.

Representative results at X-band, 8.0 GHz, are shown in Figs. 3 and 4 for samples of quartz polymide and teflon, respectively. The results, Fig. 3, employed the single vane geometry, Fig. 1c, with sample dimensions of 0.2" X 0.4". The double-vane geometry, Fig. 1d, with sample dimensions 0.4" X 0.4", was used in Fig. 4. Sample lengths were chosen such that at maximum insertion the vane(s) extend beyond the dielectric front surface. In this region (left-most two cycles in Figs. 3 and 4), the variation $\Gamma(\ell)$ is that of "empty waveguide", indicating that the cutoff conditions are well satisfied.

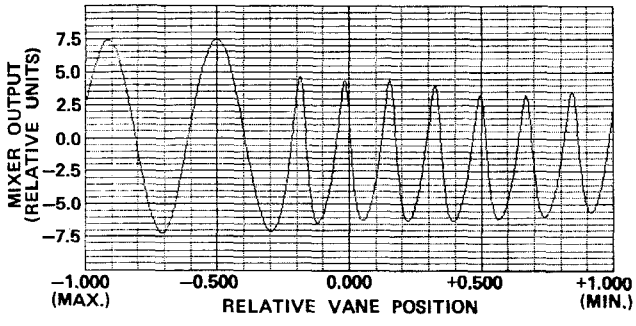

Fig. 3. Mixer output versus vane position for a split quartz polymide sample (Fig. 1c) at 8.0 GHz. Relative vane positions $\lesssim$ -0.2 correspond to the vane behind the dielectric-empty waveguide interface.

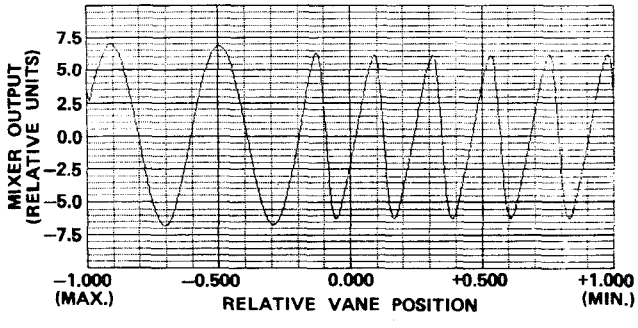

Fig. 4. Mixer output versus vane position for a centered teflon sample (Fig. 1d) at 8.0 GHz. Relative vane positions $\lesssim$ -0.2 correspond to the vane behind the dielectric-empty waveguide interface.

Data Analysis

The reflection coefficient, Eq. 3, neglects dielectric loss at the vane surface. Replacing $\Gamma(\infty)$ in Eq. 3. by a complex constant $|A|e^{j\alpha}$ and fitting experimental results to determine all of the parameters will correctly determine the complex propagation constant $\gamma = \alpha + j\beta$. The complex propagation constant is analyzed in terms of the complex dielectric constant using expressions for γ in "inhomogeneously filled waveguides" [3]. Data used to determine γ must exclude vane positions near the dielectric-empty waveguide interface ($\ell_v/\lambda_g \lesssim 1/2$, Figs. 1b and 1c.) Higher order modes excited at the discontinuity must be completly damped out in the data region analyzed.

The reflection coefficient for the centered dielectric, Fig. 1d, has been determined using a normal

mode expansion for the fields in each region. The boundary conditions at the empty guide-dielectric and vane interfaces are satisfied simultaneously by using the Least-Squares Boundary Residual Method [4]. Equations for the normal mode coefficients in just the empty-guide region are obtained and solved using standard numerical techniques. The dependance, $\Gamma(\ell)$, calculated for different values of ε' and tan δ is compared with the measured variation. The parameters ε' and tan δ are iteratively adjusted to minimize the variance.

Discussion

The automated Moving Vane Dielectometer provides a rapid measurement of reflection coefficient as a function of sample length from which the complex dielectric constant is determined. Several factors limiting accuracy in slotted line measurements are eliminated. These include 1) non-square law detector response, 2) sample length uncertainties, and 3) sample-waveguide termination uncertainties. Applied to measurements of dielectric constants versus temperature, sample length thermal expansion corrections are not required. This system should be particularly useful in the investigation of dielectric constant inhomogenities such as do occur in artificial dielectric metal-foam lense materials. Application of this technique at 8 millimeters is expected to be straight-forward.

References

(1) Technique of Microwave Measurements, Ch. 10, "The Measurement of Dielectric Constants." Carol G. Montgomery, Ed. (M.I.T. Rad. Lab. Series, Vol. 11, Boston Technical Lithographers, Inc., Lexington, Mass., 1963).

(2) Microwave Transmission Design Data, Theodore Moreno (Dover Publications, Inc., New York, 1958), p. 140.

(3) Field Theory of Guided Waves, Robert E. Collin, Ch. 6 (McGraw-Hill, New York, 1960), p. 228.

(4) J. Brian Davies, IEEE Trans. MTT, MTT-21, 99(1973)